

Phase Diagram Investigation and Proposition of a Thermodynamic Evaluation of the Tin-Selenium System

Y. Feutelais, M. Majid, and B. Legendre

Laboratoire de Chimie Physique Minérale et Bioinorganique UA 401

Faculté de Pharmacie

5 rue J.-B. Clément, F-92296 Châtenay-Mal abry, France

and

S.G. Fries

Lehrstuhl für Theoretische Hüttenkunde

RWTH-Aachen, Kopernikusstr. 16, D-52056 Aachen, Germany

(Submitted December 1, 1995)

Differential scanning calorimetry (DSC) and x-ray diffraction (XRD) measurements provide phase diagram data in the whole composition range. From the results and literature data, an optimization and calculation study was done to generate the thermodynamic functions of each phase.

Introduction

According to the assessment of [86Sha], the phase diagram for the Sn-Se binary system shows two intermediate stoichiometric compounds, SnSe with low (α SnSe) and high (β SnSe) temperature forms and SnSe₂, and a monotectic invariant on the Sn-rich side. Whereas, the general shape of the phase diagram seems to be established, some problems remain concerning the melting points of the compounds and the order of transition in SnSe.

Liquid thermodynamic data available in the literature show a large negative departure from ideality with a characteristic shape indicating the presence of short-range order. A thermodynamic evaluation of the system is presented using the optimization and calculation program of [77Luk] and [92Luk].

Experimental Investigation

Experimental Details

Twenty-eight alloys were carefully weighed from pure Sn (Fluka, 6N, Fluka, L'Isle d'Abeau Chesnes BP 701, F-38297 St-Quentin Fallavier Cedex, France) and pure Se (Aldrich, 5N, Sigma-Aldrich-Chimie, L'Isle d'Abeau Chesnes BP 701, F38297 St-Quentin Fallavier Cedex, France). Nonsoluble impurities were removed from Sn by filtration under purified argon on silica wool. Because the high vapor pressure of Se voids preparation of alloys by direct melting, special attention was paid to the procedure for alloy preparation.

To prevent oxidation, the pure elements were placed in a silica tube (5 mm inside diameter, 6 mm outside diameter, 25 mm length), which was then sealed under vacuum (10^{-1} Pa). The total weights mixed were approximately 0.200 g.

The alloys were then subjected to the following heat treatment in a furnace that had the capacity of controlling temperatures

up to 1200 °C and maintaining temperature uniformity to ± 0.5 °C: (1) 24 h at 250 °C, (2) slow heating until 500 °C followed by 24 h annealing, (3) slow heating until 900 °C (≈ 20 °C above the temperature of fusion of SnSe) for alloys with $X_{\text{Se}} < 0.55$ or until 700 °C (≈ 50 °C above the temperature of fusion of SnSe₂) for alloys with $X_{\text{Se}} < 0.55$, (4) to remove any possible remaining condensed vapor, the alloys were then introduced into a Netzsch DTA apparatus (Netzsch-Frères, 32-34 Avenue des Chardons, F-77340 Pontault-Combault, France) equipped with a "low head" to obtain a gradient of temperature, and (5) 24 h annealing at 500 °C.

DSC measurements were subsequently carried out on a DSC 121 (Setaram, 7 rue de l'Oratoire, BP 34, F-69641 Caluire Cedex, France) and a multi-HTC (Setaram) whose main characteristics are listed in Table 1. A heating rate of 1 °C/min was used except for alloys with $0.55 \leq X_{\text{Se}} \leq 0.667$ where the eutectic and the liquidus temperatures were too close together. In those cases, to get a good differentiation between the thermal arrests, the heating rate was lowered to 0.1 °C/min. Calibration of the DSC apparatus was made by checking the temperatures of fusion of In, Sn, Te, and Sb for the DSC 121 and Ag and Ge for the multi-HTC.

Identification of phases was made with powder diffraction measurements on a PW 1729 (Philips Electronique Industrielle S.A.S., Analyse Rayons X, 22 Avenue Descartes, F-94454) x-ray diffractometer (equipped with goniometer driven

Table 1 Characteristics of DSC Measurements

Characteristics	DSC 121	Multi-HTC
Temperature range.....	-120 to 830 °C	20 to 1600 °C
Sensitivity	5 to 15 μ V	500 μ V
Heating and cooling rate	0.01 to 30 °C/min	0.01 to 30 °C/min

Table 2 Experimental Phase Diagram Data Obtained in This Work

X_{Se} , at. %	Temperature, °C				Identification of phases at room temperature
	Liquidus	Solidus	Invariants		
10.0	775.6	...	231.7	526.7	$\beta\text{Sn} + \alpha\text{SnSe}$
20.0	822.7	...	231.7	526.8	$\beta\text{Sn} + \alpha\text{SnSe}$
25.0	831.4	...	231.6	526.7	$\beta\text{Sn} + \alpha\text{SnSe}$
30.0	231.5	526.0	$\beta\text{Sn} + \alpha\text{SnSe}$
35.0	231.5	526.0	$\beta\text{Sn} + \alpha\text{SnSe}$
40.0	231.5	526.0	$\beta\text{Sn} + \alpha\text{SnSe}$
45.0	231.7	526.5	$\beta\text{Sn} + \alpha\text{SnSe}$
49.0	865.5	...	231.6	526.1	$\beta\text{Sn} + \alpha\text{SnSe}$
49.5	871.5	524.3	231.7	831.6	$\beta\text{Sn} + \alpha\text{SnSe}$
50.0	...	521.1	872.5		αSnSe
50.5	870.9	521.0	629.1		$\alpha\text{SnSe} + \text{SnSe}_2$
51.0	865.0	521.1	629.4		$\alpha\text{SnSe} + \text{SnSe}_2$
53.0	520.4	628.9	$\alpha\text{SnSe} + \text{SnSe}_2$
55.0	793.6	...	520.6	629.5	$\alpha\text{SnSe} + \text{SnSe}_2$
56.0	770.5	...	519.7	629.9	$\alpha\text{SnSe} + \text{SnSe}_2$
57.0	744.4	...	520.0	628.7	$\alpha\text{SnSe} + \text{SnSe}_2$
58.0	722.0	...	520.0	628.7	$\alpha\text{SnSe} + \text{SnSe}_2$
59.0	690.0	...	518.9	629.5	$\alpha\text{SnSe} + \text{SnSe}_2$
60.0	660.0	...	519.6	629.6	$\alpha\text{SnSe} + \text{SnSe}_2$
61.0	520.0	628.9	$\alpha\text{SnSe} + \text{SnSe}_2$
63.0	640.0	...	520.0	629.5	$\alpha\text{SnSe} + \text{SnSe}_2$
65.0	643.6	...	629.4		$\alpha\text{SnSe} + \text{SnSe}_2$
66.7	645.0		SnSe_2
70.0	642.4	...	219.9		$\text{Se} + \text{SnSe}_2$
75.0	635.0	...	219.9		$\text{Se} + \text{SnSe}_2$
80.0	624.2	...	220.0		$\text{Se} + \text{SnSe}_2$
85.0	613.8	...	219.7		$\text{Se} + \text{SnSe}_2$
90.0	599.3	...	219.9		$\text{Se} + \text{SnSe}_2$

by a software developed by [95Fra]) using the K_{α_1} radiation of copper ($\lambda_{\text{Cu}K_{\alpha_1}} = 1.5405 \text{ \AA}$).

Results

Liquidus and Invariant Temperatures, Enthalpy of Fusion, Temperature

Table 2 gives the temperatures of both liquidus and invariants, whereas Table 3 presents the measured temperatures and enthalpies of fusion of the compounds available in the literature. The melting temperature obtained for the intermetallic compound βSnSe is 1145.65 K, which agrees well with the most recently reported value [94Yam]. The present value for the enthalpy of fusion, $\Delta_{\text{fus}}H = 14 \pm 1 \text{ kJ/g-atom}$, is 15 to 20% lower than the reported values of [81Bal] and [94Yam], which were obtained from heat content measurements. Both of those investigations used the drop calorimetric method and thus worked with open tubes. Because Se is a volatile element, some evaporation would yield an overestimation of the heat effect.

The melting temperature obtained for SnSe_2 is 918.15 K with $\Delta_{\text{fus}}H = 17 \pm 1 \text{ kJ/g-atom}$, which is much lower than the value given by [82Ale], who gave no information on the method for this determination.

Invariants

The calorimetric study of the invariants led to the invariant equilibria listed in Table 4.

Phase Transition in SnSe

According to the assessment of [86Sha] and as shown in Table 5, all workers agree with the presence of a phase transformation at $X_{\text{Se}} = 0.500$. There is conflicting evidence with regard to the phase transition in SnSe, and doubt remains as to the order of this transition. The works of [81Bal] and [94Yam] reveal the presence of a small latent heat at the transition temperature, which seems to indicate a first-order transition in the sense of Ehrenfest and Landau. On the contrary, the continuous variation of the primary order parameter with temperature obtained by neutron diffraction measurements [86Cha] is more typical of a second-order transition. Still, the sharp decrease of this order parameter in the transition temperature range may be interpreted as a first-order transition with order parameter [67Lan, 81Wey]. These data have to be compared with the structural results of [81Sch], who concluded from their XRD measurements that there is an indication of a possible first-order transition near the critical temperature for the λ -type phase transition.

We found invariant reactions on both sides of the composition, $X_{\text{Se}} = 0.500$ at different temperatures. Verification was made

Section I: Basic and Applied Research

Table 3 Temperature and Enthalpy of Fusion of $\beta\text{Sn}_{0.5}\text{Se}_{0.5}$ and $\text{Sn}_{0.33}\text{Se}_{0.67}$

Reference	Method	$\beta\text{Sn}_{0.5}\text{Se}_{0.5}$		$\text{Sn}_{0.33}\text{Se}_{0.67}$	
		Temperature, K	$\Delta_{\text{fus}}H$, kJ/g-atom	Temperature, K	$\Delta_{\text{fus}}H$, kJ/g-atom
[06Pel, 09Pel].....	Thermal analysis	1133	...	918	...
[09Bil].....	Thermal analysis	1134	...	929	...
[66Kar].....	...	1153	...	930	...
[68Gas].....	Thermography	1153	...	948	...
[70Gla].....	Density	1133
[76Rou].....	DTA	1135	...	930	...
[77Kul].....	Vapor pressure	929 ± 2	...
[81Bal].....	Calorimetry	1135	16.4 ± 1.5
[82Ale].....	Vapor pressure	...	21 ± 4	929 ± 2	25.5
[92Liu].....	Evacuated glass capsule	1138	...	948	...
[94Yam].....	Calorimetry	1149 ± 2	17.75 ± 0.4
This work.....	DSC	1145.7	14 ± 1	918.2	17 ± 1
This work.....	Calculated	1146.9	15.8	919.8	16.2

Table 4 Sn-Se Invariant Equilibria

Type	Reaction	Temperature, °C	Comment
E1.....	$L_1 \leftrightarrow \beta\text{Sn} + \alpha\text{SnSe}$	231.7 ± 0.5	Degenerate
P1.....	$\alpha\text{SnSe} \leftrightarrow L_1 + \beta\text{SnSe}$	526.3 ± 0.5	$X_{\text{Se}}^{L_1} = 2.5$
M.....	$L_2 \leftrightarrow L_1 + \beta\text{SnSe}$	832.0 ± 0.5	$X_{\text{Se}}^{L_2} = 0.420$, $X_{\text{Se}}^{L_1} = 0.270$
E2.....	$L_2 \leftrightarrow \beta\text{SnSe} + \text{SnSe}_2$	629.3 ± 0.5	$X_{\text{Se}}^{L_2} = 0.613$
E3.....	$\beta\text{SnSe} \leftrightarrow \alpha\text{SnSe} + \text{SnSe}_2$	520.2 ± 0.5	...
E4.....	$L_2 \leftrightarrow \text{SnSe}_2 + \text{Se}$	219.9 ± 0.5	Degenerate

by checking the variation of the invariant temperatures with different heating rates (Table 6).

The small variations in temperature with different heating rates are within the instrumental error range. Thus, two possibilities arise as to the representation of the phase diagram in the vicinity of $X_{\text{Se}} = 0.500$. Figure 1(a) shows first-order transition of the SnSe phase involving metatectic and eutectoid invariants. Figure 1(b) shows reaction between two different phases involving peritectic and eutectoid invariants.

As shown in Table 2, a thermal arrest was found with slightly decreasing temperature from 524.3 to 521.0 °C when X_{Se} increases from 0.495 to 0.510. This temperature variation seems difficult to interpret in Fig. 1(a), but may appear as the Sn-rich border of the two-phase field $\alpha\text{SnSe} + \beta\text{SnSe}$ in Fig. 1(b).

This interpretation agrees well with the results of [63Dem] and [81Bal], who gave a range of temperature for the transition instead of a definite value. We believe we cannot deal with a phase transition, but with two different phases involving peritectic and eutectoid invariants (according to Fig. 1b), whose compositions are, respectively, $0.490 < X_{\text{Se}}^I < 0.495$ and $0.510 < X_{\text{Se}}^II < 0.530$.

The composition range of both phases, αSnSe and βSnSe , are approximately 2 to 3% at the temperature of the invariants. From XRD patterns, we calculated the parameters of the or-

Table 5 Transition Temperature and Transition Order in αSnSe to βSnSe

Reference	Method	Temperature, °C	Transition order
[61Zhd].....	Dilatometry	541	Second
[63Dem].....	DTA, XRD in temperature	520 to 550	Second
[66Kar].....	Thermal analysis	540	...
[74Bla1].....	Drop calorimetry	514	...
[74Bla2].....	DTA	514	...
[76Rou].....	DTA	530	...
[79Wie].....	XRD in temperature	524 ± 5	Second
[81Bal].....	Drop calorimetry	489 to 566	First
[86Cha].....	Neutron diffraction	...	Second
[87Ras, 91Ras].....	Drop calorimetry	≈541	...
[94Yam].....	Drop calorimetry	515 ± 2	First
This work.....	DSC	Two invariants 520.2 and 526.3	...

thorhombic cell of αSnSe for three compositions, $X_{\text{Se}} = 0.450$, 0.500, and 0.550. The values observed are identical within the experimental error. Thus, a significant composition range for this phase at room temperature could not be established.

Phase Sn_2Se_3

The DSC curves carried out at composition $X_{\text{Se}} = 0.600$ did not show any more thermal arrest than those related to the invariants, E2, E3, and the liquidus. Phase Sn_2Se_3 does not undergo a phase transition. XRD patterns in this composition range, showing only the presence of the two phases, αSnSe and SnSe_2 , confirm the results of differential calorimetry. This result agrees well with the conclusion of the thermal, metallographic, and XRD study [06Pel, 66Kar], the Mössbauer works [70Bol, 71Bar], the nuclear γ -resonance investigation [71Mel], and the DTA contribution [76Rou], which did not include this compound. Sn_2Se_3 may possibly exist in a metastable state in thin films, as reported by [54Pal] from XRD results.

Table 6 Comparison of Sn-Se Invariant Temperatures with Heating Rates

Heating rate, °C/min	Invariant temperature, °C	
	Alloy $X_{Se} = 0.490$	Alloy $X_{Se} = 0.580$
0.5	526.5	520.0
1.0	526.0	520.0
2.0	526.1	519.6

Optimization and Calculation

Phase Diagram Data

In earlier works, [06Pel] and [09Pel] claimed the existence of SnSe and SnSe₂ and gave some liquidus points and melting temperatures of these two compounds. The first complete shape of the liquidus was established by [09Bil], whose interpretation points out the existence of compound Sn₂Se₃. Later, using hardness measurements and crystal growth, [38Jen] found a solubility of Se in βSn of 0.05 at.% at 200 °C. From electrical measurements, [63Alb] gave the composition limits of stability at the Se-rich side for αSnSe as 50.005 at.% at 300 °C and 50.01 at.% at 400 °C. A solubility curve of Se in Sn for 300 to 550 °C is proposed by [64Vas], who used a diffusion method. The first description of the whole phase diagram including the monotectic invariant was given by [66Kar], who used metallography, XRD, and DTA investigations. More recently, from measurements on enthalpy as a function of composition and DSC, [87Kot] confirmed the general shape of the description given by [66Kar]. The melting temperature of the two compounds are presented in the section, "Experimental Investigation" (Table 3).

Enthalpy Data

The enthalpies of mixing in the liquid state were studied by [87Kot], who reported results for six temperatures from 921 to 1243 K. As explained by these authors, the large negative enthalpy of formation (−45 kJ/g-atom at $T = 1175$ K) located at $X_{Se} = 0.5$ indicates the presence of short-range order based on βSnSe.

Heat content measurements on alloys of composition $X_{Se} = 0.500$ carried out by different authors [74Blal, 81Bal, 91Ras, 94Yam] are in good agreement for the low-temperature phase. For the high-temperature modification, the slope of the curve $H(T) - H(298.15) = f(T)$ given by [91Ras] is less pronounced than those of other authors. Only [77Kul] provided heat content results for SnSe₂ but with no indication of the experimental method used.

In a careful study, [81Wie] determined the heat capacities of both compounds in the temperature range from 230 to 580 K using DSC. More recently, [88Ras] reported a few C_p values for αSnSe in the range from 300 to 800 K, which show a bigger temperature dependence than the measured values of [81Wie]. Because [88Ras] did not give any experimental information, these data were not used in this optimization.

The enthalpies of formation of both compounds, αSnSe and SnSe₂, have been measured by different techniques: direct combination calorimetry [60Haj, 70Haj, 92Boo], Knudsen effusion [64Col], dissociation pressure [67Kar], emf measure-

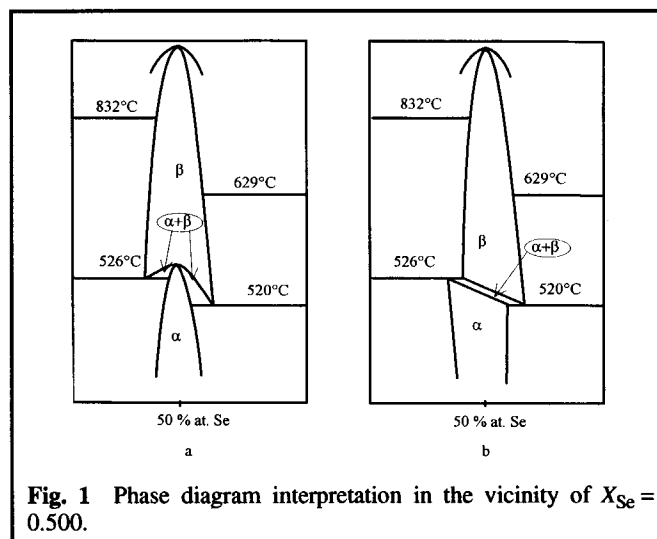


Fig. 1 Phase diagram interpretation in the vicinity of $X_{Se} = 0.500$.

ments [71Mel] for αSnSe and direct combination calorimetry [92Boo], equilibrium data [67Rau], dissociation pressure [67Kar, 77Kul] for βSnSe. If the values are in relatively good agreement for αSnSe, the enthalpy of formation of SnSe₂ coming from dissociation pressure is 20% higher [67Kar] or 12% lower [77Kul] than the average value of the other authors.

Gibbs Energy Data

Because of the high temperature of fusion of αSnSe and the high vapor pressure of Se at high temperature, the only available chemical potential data were determined in the solid state by [71Mel] from emf measurements.

Previous Calculations

By applying a regular associated treatment to the melts, [88Kot] and [89Cas] showed that the liquid is better described with the use of one associate (βSnSe) instead of two (βSnSe + SnSe₂). The standard enthalpy and entropy of formation are 45.5 kJ/g-atom and 4.15 J/K·g-atom, respectively.

Analytical Description of the Phase Stabilities

Pure Elements

According to the Scientific Group Thermodata Europe (SGTE), the temperature dependence of the molar Gibbs energy of the pure stable elements, referred to standard state, is given by the following expression:

$$G_i^0 - H_i^{SER} = A + BT + C \ln T + DT^2 + ET^{-1} + FT^3 + IT^7 + JT^{-9} \quad (\text{Eq 1})$$

The coefficients of this equation, available from the database of [91Din], are given in the appendix. H_i^{SER} is the enthalpy of the pure element i at 298.15 K in its stable state.

Liquid Phase

As discussed in the section, "Enthalpy Data," the liquid phase was described using the association model presented by [82Som1] and [82Som2]. Then the Gibbs energy (given for one mole of formula units) is expressed as the sum of a refer-

Section I: Basic and Applied Research

Table 7 Data Sources Used during Final Optimization

Reference	Phase diagram	Enthalpy of fusion	Enthalpy of formation	Heat content	C_p	Enthalpy of mixing	Chemical potential
[06Pel]	×						
[09Pel]	×						
[09Bil]	×						
[64Vas].....	×						
[66Kar]	×						
[67Rau].....			×				
[71Mel].....							×
[74Bla].....				×			
[77Kul]				×			
[81Bal].....				×			
[81Wie].....					×		
[87Kot].....	×					×	
[91Ras].....				×			
[92Boo].....			×				
[94Yam].....				×			
This work.....	×	×					

ence part, G^{ref} , formation of the associate part, $\Delta_f G$, ideal part, G^{id} , and an excess part, G^{ex} :

$$G^{\text{liq}} - H^{\text{SER}} = G^{\text{ref}} + \Delta_f G + G^{\text{id,liq}} + G^{\text{ex,liq}} \quad (\text{Eq 2})$$

with:

$$G^{\text{ref}} = \left\{ X_{\text{Sn}} \cdot \left[G_{\text{Sn}}^{\text{0,liq}}(T) - H_{\text{Sn}}^{\text{SER}}(298.15) \right] \right\} + X_{\text{Se}} \cdot \left[G_{\text{Se}}^{\text{0,liq}}(T) - H_{\text{Se}}^{\text{SER}}(298.15) \right] \cdot (y_{\text{Sn}} + 2y_{\text{SnSe}} + y_{\text{Se}}) \quad (\text{Eq 3})$$

$$\Delta_f G = y_{\text{Sn}} \cdot G_{\text{Sn}}^{\text{0,liq}} + y_{\text{SnSe}} \cdot G_{\text{SnSe}}^{\text{0,liq}} + y_{\text{Se}} \cdot G_{\text{Se}}^{\text{0,liq}} \quad (\text{Eq 4})$$

$$G^{\text{id,liq}} = R \cdot T \cdot z \cdot (y_{\text{Sn}} \cdot \ln y_{\text{Sn}} + y_{\text{SnSe}} \cdot \ln y_{\text{SnSe}} + y_{\text{Se}} \cdot \ln y_{\text{Se}}) \quad (\text{Eq 5})$$

$$G^{\text{ex,liq}} = L_{\text{Sn,SnSe}}^{\text{0,liq}} \cdot y_{\text{Sn}} \cdot y_{\text{SnSe}} + L_{\text{SnSe,Se}}^{\text{0,liq}} \cdot y_{\text{SnSe}} \cdot y_{\text{Se}} + L_{\text{Sn,SnSe}}^{\text{1,liq}} \cdot y_{\text{Sn}} \cdot y_{\text{SnSe}} \cdot (y_{\text{Sn}} - y_{\text{SnSe}}) + L_{\text{SnSe,Se}}^{\text{1,liq}} \cdot y_{\text{SnSe}} \cdot y_{\text{Se}} \cdot (y_{\text{SnSe}} - y_{\text{Se}}) + L_{\text{Sn,SnSe}}^{\text{2,liq}} \cdot y_{\text{Sn}} \cdot y_{\text{SnSe}} \cdot (y_{\text{Sn}} - y_{\text{SnSe}})^2 + L_{\text{SnSe,Se}}^{\text{2,liq}} \cdot y_{\text{SnSe}} \cdot y_{\text{Se}} \cdot (y_{\text{SnSe}} - y_{\text{Se}})^2 \quad (\text{Eq 6})$$

where T is the temperature; Sn, SnSe, and Se are the three species in the liquid; y_i are their site fractions; and z is the number of lattice sites in one mole of formula units: $z = y_{\text{Sn}} + y_{\text{SnSe}} + y_{\text{Se}}$. The $L_{i,j}^{\text{liq}}$ are polynomial interaction terms described with the Redlich-Kister formalism [48Red], which can be interpreted as a modification of the polynomial description used by Margules [1895Mar]. The terms $G_i^{\text{0,liq}}$ and $L_{i,j}^{\text{liq}}$ are expressed as functions of temperature from Eq 1.

Solid Phases

As discussed in the section, "Experimental Investigation," the width of αSnSe is too small at room temperature to define significant phase limits. The reported values of [63Alb] (see section, "Phase Diagram Data") confirm the narrow range of homogeneity of this phase, but the experimental data are insufficient to enable modeling this phase as nonstoichiometric. No data were reported for the composition limits of βSnSe and SnSe_2 . Thus αSnSe , βSnSe , and SnSe_2 were treated as stoichiometric compounds. The Gibbs energy of one mole of formula units is expressed as:

$$G_{\text{p}}^{\text{Sn}_p\text{Se}_q} - p \cdot H_{\text{Sn}}^{\text{SER}} - q \cdot H_{\text{Se}}^{\text{SER}} = A + BT + C \ln T + DT^2 + ET^{-1} + FT^3 \quad (\text{Eq 7})$$

where p and q denote the stoichiometric numbers.

The coefficients were fitted to the experimental data (384 data were used) by a least squares technique described and programmed (BINGSS) by [77Luk]. Table 7 gives the data sources used in the final data set.

Results and Discussion

One of the problems encountered in the optimization was the definition of the stoichiometry of the two solid phases αSnSe and βSnSe . According to our experimental results, we made the following approximations.

Since the widths of these phases at the invariant temperatures extend on both sides of the composition $X_{\text{Se}} = 0.500$, we chose the stoichiometric composition $\text{Sn}_{0.5}\text{Se}_{0.5}$ for both α and β .

Then came the problem of the phase transformation temperature. With the assumption of the same composition for α and β , it is not possible, from a thermodynamic point of view, to state two different temperatures for the phase transition. Thus we

Table 8 Optimized Coefficients According to the Analytical Description of the Phases

Function	A	B	C	D	E	F
$G_{\text{SnSe}}^{0,\text{liq}}$	-134 591.86	278.59972	-32.99			
$L_{\text{Sn,SnSe}}^{0,\text{liq}}$	43 462.43	-21.60740				
$L_{\text{SnSe,Se}}^{0,\text{liq}}$	15 432.80	-19.06391				
$L_{\text{Sn,SnSe}}^{1,\text{liq}}$	-1 032.50					
$L_{\text{SnSe,Se}}^{1,\text{liq}}$	-8 995.55					
$G(\alpha\text{SnSe}) - H_{\text{Sn}}^{\text{SER}} - H_{\text{Se}}^{\text{SER}}$	-63 171.87	134.4964	-26.31	-1.82	61 422.50	0.11076
$G(\beta\text{SnSe}) - H_{\text{Sn}}^{\text{SER}} - H_{\text{Se}}^{\text{SER}}$	-62 529.58	133.69002	-26.31	-1.82	61 422.50	0.11076
$G(\text{Sn}_1\text{Se}_2) - H_{\text{Sn}}^{\text{SER}} - 2 \cdot H_{\text{Se}}^{\text{SER}}$	-46 104.05	121.16205	-24.84	-1.64	39 347.00	0.1185733

Note: Functions are expressed in J/g-atom.

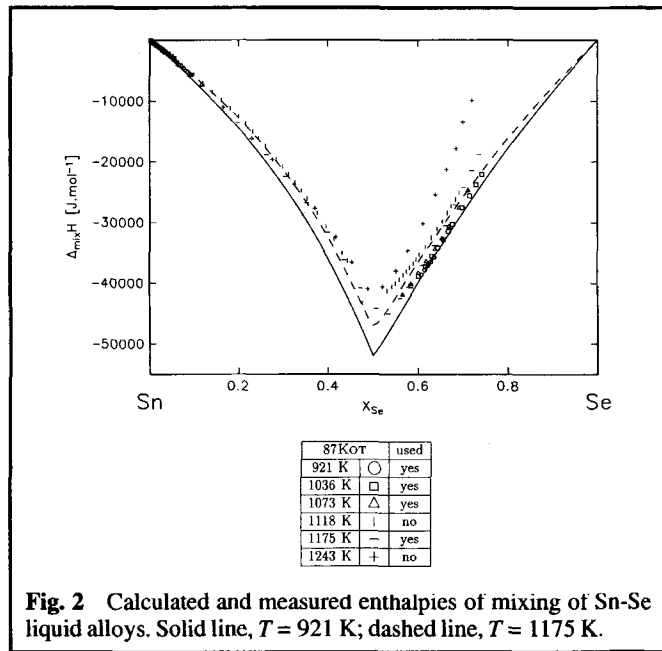


Fig. 2 Calculated and measured enthalpies of mixing of Sn-Se liquid alloys. Solid line, $T = 921$ K; dashed line, $T = 1175$ K.

defined a hypothetical transformation temperature as $T_{\text{trans}} = (T_{\text{P1}} + T_{\text{E3}})/2$ ($T_{\text{trans}} = 523.35$ °C).

Heat capacity data are available [81Wie] only for α . To get homogeneous descriptions of the Gibbs functions for both phases, C_p coefficients of β were constrained during the optimization to be the same as for α .

The optimized coefficients are given in Table 8.

The associate model defines a fixed C_p that just depends on the definition of the associate. This value is intrinsic and cannot be adjusted. To fit the results found for the enthalpy of mixing [87Kot] for various temperatures, an extra C_p term was optimized in the description of the Gibbs energy of formation of the associate. We always got a significantly lower mean square of errors by removing the data obtained for the highest temperature (1243 K). The high vapor pressure of Se and compounds may suggest evaporation problems for this temperature, and the related data were removed from the final data set. Moreover, we did not include the data for $T = 1118$ K because they show a less negative departure from ideality than the values measured at $T = 1175$ K; this would introduce a

negative excess C_p . As shown in Fig. 2, the calculated enthalpies of mixing (921 and 1175 K) are in good agreement with the experimental data. The convexity shown by the two parts of these curves have to be compared to the endothermic values of the enthalpic terms $L_{\text{Sn,SnSe}}^{0,\text{liq}}$ and $L_{\text{SnSe,Se}}^{0,\text{liq}}$ (Table 8), which indicate repulsion between the associate and the pure elements. The consequence in the phase diagram is the presence of a miscibility gap in the Sn-rich portion and of a flat liquidus in the Se-rich region. The degree of association, which is 99.7% at 921 K and 97.4% at 1175 K, decreases slowly with temperature. This confirms the presence of strong interactions in this system, as shown by [88Kot] and [89Cas].

In the optimization of the parameters of solid phases, we first assumed a constant C_p term and obtained values for coefficients A, B, and C (Eq 7). Then, since heat capacity data were available, the temperature dependence of C_p could be described by optimizing coefficients D, E, and F of Eq 7. During this step, all the other parameters were fixed, and only the C_p data of [81Wie] were used. As shown in Fig. 3 and 4, the calculated heat capacities of both phases are in excellent agreement with the experimental values.

The heat content calculations are in very good agreement with the available data (Fig. 5 and 6). With the assumption made for the description of phases α and β , the calculated heat of transformation is 640 J/mol in accordance with the estimated values of [81Bal] (800 J/g-atom) and [94Yam] (600 J/g-atom). The good fit of the heat content in the liquid phase indicates a good consistency between the heat content data and the temperature dependence of the enthalpies of mixing.

The use of the temperature and enthalpy of fusion given by [82Ale] for SnSe_2 led to a worse description of the phase diagram and heat content of phases. Thus, these values were not used in the final optimization. The calculated enthalpy of fusion of the two compounds, given in Table 3, are in fair agreement with the used data.

Several runs of optimization were tried with the different enthalpy of formation data given in the literature. (See "Enthalpy Data.") The values of [67Rau], [71Mel], and [92Boo] showed the best consistency with all the other data and were used in the final optimization. The result of the calculation gave a reasonable agreement with the experimental enthalpy of formation as shown in Table 9.

Section I: Basic and Applied Research

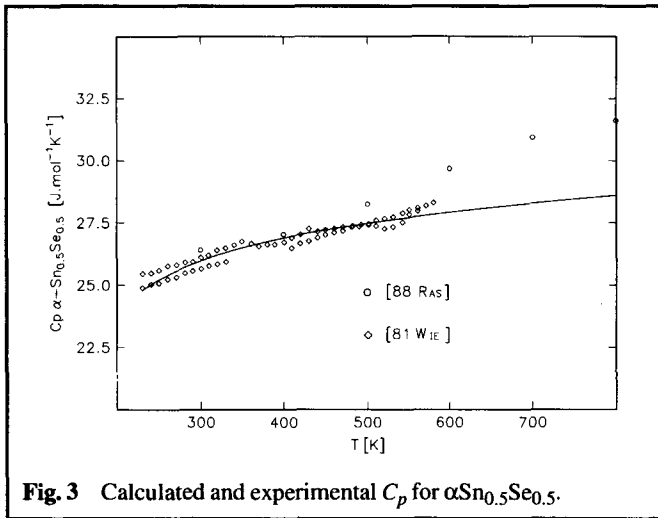


Fig. 3 Calculated and experimental C_p for $\alpha\text{Sn}_{0.5}\text{Se}_{0.5}$.

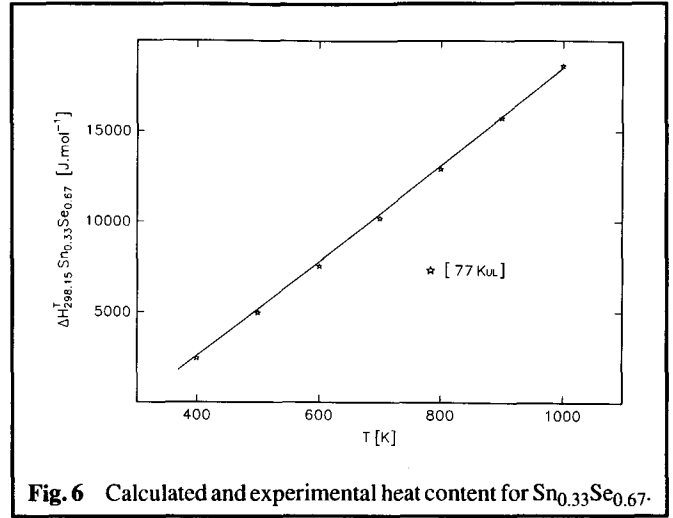


Fig. 6 Calculated and experimental heat content for $\text{Sn}_{0.33}\text{Se}_{0.67}$.

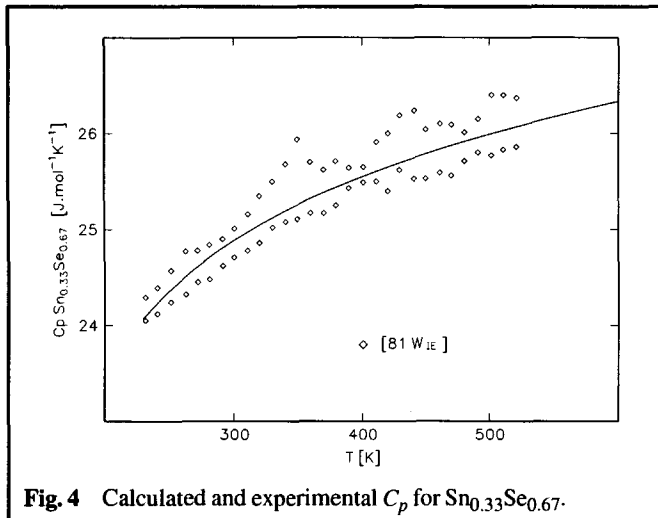


Fig. 4 Calculated and experimental C_p for $\text{Sn}_{0.33}\text{Se}_{0.67}$.

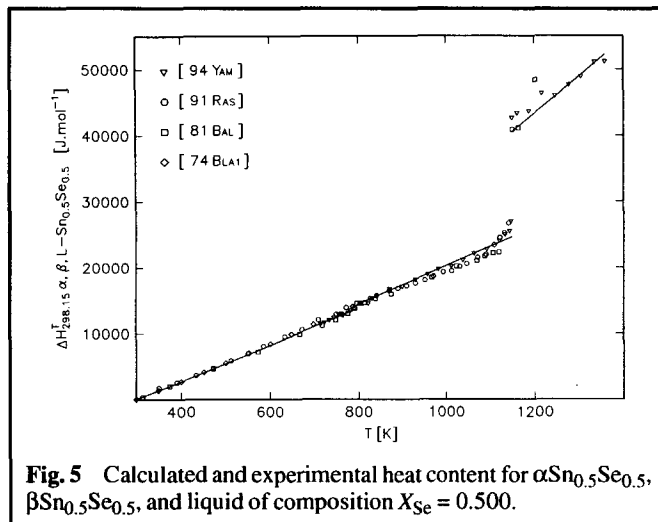


Fig. 5 Calculated and experimental heat content for $\alpha\text{Sn}_{0.5}\text{Se}_{0.5}$, $\beta\text{Sn}_{0.5}\text{Se}_{0.5}$, and liquid of composition $X_{\text{Se}} = 0.500$.

fair agreement with the calculation. Since there is no two-phase field, $\alpha\text{SnSe} + \beta\text{SnSe}$, and because these two phases have the same stoichiometric composition, Fig. 7 does not show any three-phase equilibrium point for the transformation temperature. For this temperature ($T = 796.5 \text{ K}$), we have the following equality: $\mu_{\text{Sn}}^{\text{L1}} = \mu_{\text{Sn}}^{\alpha\text{SnSe}} = \mu_{\text{Sn}}^{\beta\text{SnSe}} = \mu_{\text{Sn}}^{\text{SnSe}_2}$. We have an apparent four-phase equilibrium in contradiction with the phase rule. But, this is only a consequence of the coincidence of the phase transformation temperatures according to the above-mentioned approximations. In fact, at $T = 796.5 \text{ K}$, we have the two following equilibria: $\alpha\text{SnSe} \leftrightarrow \text{L1} + \beta\text{SnSe}$ and $\beta\text{SnSe} \leftrightarrow \alpha\text{SnSe} + \text{SnSe}_2$.

The results of the phase diagram calculation together with the experimental data are given in Fig. 8. The liquidus data of [66Kar] on the Se-rich side, being very different from the values of the other authors, were not used in the final optimization run. Contamination of elements is not an explanation as the degenerate invariant temperature on the Se side is in fair agreement with the other reported values. An explanation may be proposed after looking at the DTA curve given in the publication: the liquidus temperature does not seem to correspond to the end of melting, and thus the liquidus temperature may be underestimated. As shown in Table 3, some divergence occurs in the temperatures of fusion of the two compounds. In order to avoid getting an average value, we chose to use our experimental measurements, which were included with a normal weight to be sure not to force the optimization to fit our data. The same treatment was applied to the monotectic invariant for which some differences can be found in the temperature. Figure 8 shows that the optimized phase diagram fits the data well. The two invariants related to the transformation $\alpha\text{SnSe} \rightarrow \beta\text{SnSe}$ are given by dashed lines for the reasons explained above. We included in Table 10 experimental and calculated invariants obtained in phase diagram investigations. The reported transformation temperatures of $\alpha\text{SnSe} \rightarrow \beta\text{SnSe}$ are given in Table 5. The calculated critical temperature of the miscibility gap, 1141 K, is in reasonable agreement with the proposed value of [87Kot] (1114 K).

In Fig. 7, the calculated Sn partial Gibbs energies of the two-phase fields are plotted. The measured values of [71Mel] are in

Summary

DSC analysis and XRD investigation provide a reaction between phases instead of a phase transition around the composition $X_{Se} = 0.500$. Nevertheless, the lack of experimental data defining the narrow range of solubility of both phases made it necessary to assume the phases as stoichiometric with the same stoichiometry. The good agreement observed between the calculated results and the literature experimental values validates the assumption. Considering the difficulty in obtaining valuable experimental data on the concentration range of phases αSnSe and βSnSe and in determining the kind of defects that enable the deviation from the ideal composition, the thermodynamic description presented here seems to represent a fair modeling of the experimentally determined properties of this system.

Acknowledgments

The authors thank H.L. Lukas for supplying the programs, additional information on how to use them, and helpful discussions.

Cited References

1895Mar: M. Margules, "About the Composition of Saturated Vapor Mixtures," *Sitzungsber. Akad. Wiss. Wien, Mathem. Naturwiss. Kl. 2a*, 104, 1243-1278 (1895) in German.

06Pel: H. Pelabon, "On the Sulfides, Selenides and Tellurides of Tin," *Compt. Rend.*, 142, 1147-1149 (1906) in French.

09Bil: W. Biltz and W. Werner, "A Study of the Phase Diagram of Sn with S, Se and Te," *Z. Anorg. Chem.*, 64, 226-235 (1909) in German.

09Pel: H. Pelabon, "On the Fusibility of Alloys of Sulfur, Selenium and Tellurium with Some Metal," *Ann. Chim. Phys.*, 17 526-566 (1909) in French.

38Jen: E. Jenckel and L. Roth, "The Solubility of a Few Metals in Tin and Their Effect Upon the Recovery Temperature," *Z. Metallkd.*, 30(4), 135-144 (1938) in German.

48Red: O. Redlich and A. Kister, "Thermodynamics of Nonelectrolyte Solutions. Algebraic Representation of Thermodynamic Properties and the Classification of Solutions," *Ind. Eng. Chem.*, 40, 345-348 (1948).

54Pal: M.S. Palatnik and V.V. Levitin, "X-Ray Diffraction Studies of Tin-Selenium, Zinc-Selenium, Cadmium-Selenium and Silver-Selenium Alloys," *Dokl. Akad. Nauk SSSR*, 96(5), 975-978 (1954) in Russian.

60Haj: S.N. Hajiev and K.A. Sharifov, "Determination of Heat of Formation of Tin Selenide Formed in the Calorimeter Bomb," *Dokl. Akad. Nauk Azerb. SSR*, 16, 659-662 (1960) in Russian.

61Zhd: V.V. Zhdanova, "A Phase Transition of the Second Kind in SnSe," *Fiz. Tverd. Tela.*, 3(5), 1619-1620 (1961) in Russian; TR: *Sov. Phys. Solid State*, 3(5), 1174-1175 (1961).

63Alb: W. Albers, C. Haas, and H.J. Vink, "Quenching Effects and the Determination of the Existence Region of Semiconducting Compounds," *Philips Res. Rept.*, 18, 372-376 (1963).

63Dem: S.A. Dembovskii, B.N. Egorov, A.S. Pashinkin, and Y.A. Polyakov, "Phase Transformation of the Second Order in SnSe," *Zh. Neorg. Khim.*, 8(4), 1025-1026 (1963) in Russian; TR: *Russ. J. Inorganic Mater.*, 8(4), 530-531 (1963).

64Col: R. Colin and J. Drowart, "Thermodynamic Study of Tin Selenide and Tin Telluride Using a Mass Spectrometer," *J. Trans. Faraday Soc.*, 60, 673-683 (1964).

64Vas: T.V. Vasilenko and Y.I. Khar'kov, "Diffusion and Solubility of Selenium in Molten Tin," *Fiz. Metal. Metalloved.*, 18(2), 203-209 (1964) in Russian; TR: *Phys. Met. Metallogr.*, 18(2), 45-50 (1964).

Table 9 Calculated and Experimental Enthalpy of Formation

Reference	Used in final optimization	$\Delta_f H_{\text{SnSe}}^0$ (298 K), kJ/g-atom	$\Delta_f H_{\text{SnSe}_2}^0$ (298 K), kJ/g-atom
[60Haj, 70Haj].....	No	-45.5 ± 2	...
[64Col].....	No	-45 ± 3.5	...
[67Kar].....	No	-44.8 ± 0.2	-51.0 ± 3
[67Rau].....	Yes	...	-40.3 ± 2.7
[71Mel].....	Yes	-47.5 ± 1	-41.5 ± 0.4
[77Kul].....	No	...	-36.3 ± 7
[92Boo].....	No	-47.0 ± 1.5	-42.3 ± 0.5
This work calculated	...	-54.7	-34.9

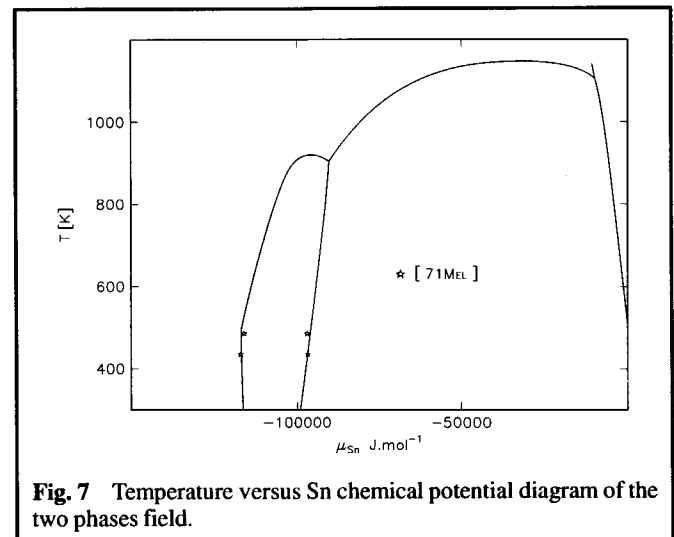


Fig. 7 Temperature versus Sn chemical potential diagram of the two phases field.

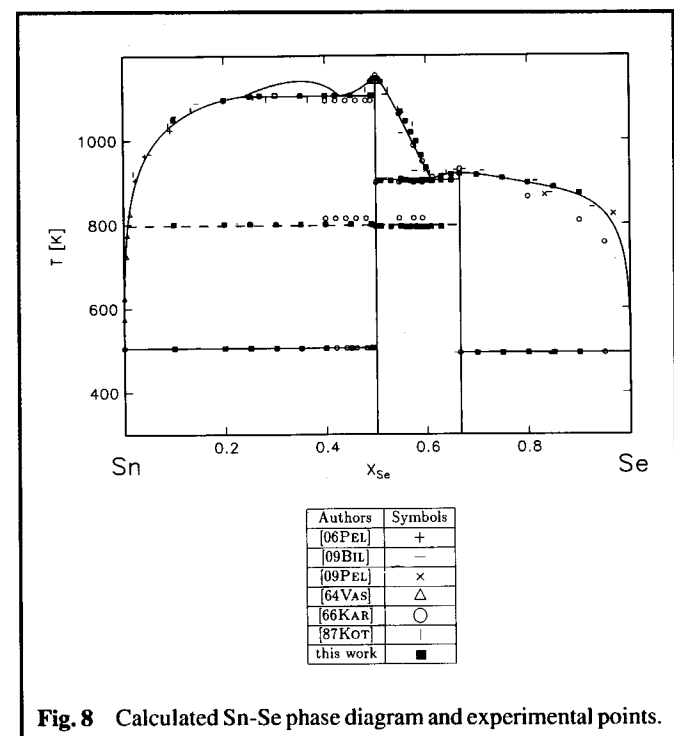


Fig. 8 Calculated Sn-Se phase diagram and experimental points.

Section I: Basic and Applied Research

Appendix

Table 10 Experimental and Calculated Invariants in the Sn-Se Phase Diagram

Phase	X_{Se}	Temperature, K		Reference
$L_1 \leftrightarrow \beta Sn + \alpha SnSe$	Degenerate	506		[09Bil]
	Degenerate	505		[66Kar]
	Degenerate	505		[76Rou]
	Degenerate	505		[87Kot]
	Degenerate	504.9		This work experimental
$\alpha SnSe \leftrightarrow L_1 + \beta SnSe$	813		[66Kar]
	...	803		[76Rou]
	0.025	799.5		This work experimental
	0.008	796.5		This work calculated
$L_2 \leftrightarrow L_1 + \beta SnSe$	0.49	1093		[66Kar]
	...	1103		[76Rou]
	...	1095		[82Ale]
	0.193 and 0.463	1094		[87Kot]
	0.270 and 0.420	1105		This work experimental
	0.239 and 0.429	1104.1		This work calculated
	$L_2 \leftrightarrow \beta SnSe + SnSe_2$	0.60	909.5	
0.61		898		[66Kar]
...		903		[76Rou]
...		911		[82Ale]
0.617		905		[87Kot]
0.613		902.5		This work experimental
0.611		903.9		This work calculated
$\beta SnSe \leftrightarrow \alpha SnSe + SnSe_2$	813		[66Kar]
	...	803		[76Rou]
	...	793.4		This work experimental
	...	796.5		This work calculated
$L_2 \leftrightarrow SnSe_2 + Se$	Degenerate	493		[09Bil]
	Degenerate	493		[66Kar]
	Degenerate	493		[76Rou]
	Degenerate	493		[87Kot]

66Kar: M.I. Karakhanova, A.S. Pashinkin, and A.V. Novoselova, "On the Fusibility Diagram of the Tin-Selenium System," *Izv. Akad. Nauk SSSR, Neorg. Mater.*, 2, 1186-1189 (1966) in Russian.

67Kar: M.I. Karakhanova, A.S. Pashinkin, and A.V. Novoselova, "Determining the Dissociation Pressure of Solid Tin Diselenide," *Izv. Akad. Nauk SSSR, Neorg. Mater.*, 3(9), 1550-1554 (1967) in Russian; TR: *Inorganic Mater.*, 3(9), 1352-1355 (1967).

67Lan: L. Landau and E. Lifchitz, "Statistical Physics," *Editions Mir*, Moscow (1967) in French.

67Rau: H. Rau, "Equilibrium Formation of H_2Se ," *Ber. Bunsenges. Phys. Chem.*, 71(7), 716-719 (1967) in German.

68Gas: A.M. Gas'kov, V.P. Zlomanov, Y.A. Sapozhnikov, and A.V. Novoselova, "The Tin-Selenium Phase Diagram," *Vestn. Mosk. Univ.*

Table 11 Phase Stabilities of Sn and Se [91Din]

Phase	Temperature, K	$G_{m,i} = f(T)$
Sn BCT_A5	100.00 to 250.00	$G_{Sn}^{0,BCT_A5} - H_{Sn}^{SER} = -7958.517 + 122.765451T - 25.8587\ln T + 0.00051185T^2 - 3.192767 \times 10^{-6}T^3 + 18.440T^{-1}$
	250.00 to 505.078	$G_{Sn}^{0,BCT_A5} - H_{Sn}^{SER} = -5855.135 + 65.443315T - 15.96117\ln T - 0.0188702T^2 + 3.121167 \times 10^{-6}T^3 - 61.960T^{-1}$
	505.078 to 800.00	$G_{Sn}^{0,BCT_A5} - H_{Sn}^{SER} = 2524.724 + 4.005269T - 8.25904867\ln T - 0.016814429T^2 + (2.623131 \times 10^{-6})T^3 - 1.081244T^{-1} - 1.2307 \times 10^{25}T^{-9}$
Sn LIQ	100.00 to 250.00	$G_{Sn}^{0,LIQ} - H_{Sn}^{SER} = -855.425 + 108.677684T - 25.85817\ln T + 0.00051185T^2 - 3.192767 \times 10^{-6}T^3 + 18.440T^{-1} + 1.47031 \times 10^{-18}T^7$
	250.00 to 505.078	$G_{Sn}^{0,LIQ} - H_{Sn}^{SER} = 1247.957 + 51.355548T - 15.9617\ln T - 0.0188702T^2 + 3.121167 \times 10^{-6}T^3 - 61.960T^{-1} + 1.47031 \times 10^{-18}T^7$
	505.078 to 800.00	$G_{Sn}^{0,LIQ} - H_{Sn}^{SER} = 9496.31 - 9.809114T - 8.25904861\ln T - 0.016814429T^2 + (2.623131 \times 10^{-6})T^3 - 1.081244T^{-1}$
Se HEX_A8	800.00 to 3000.00	$G_{Sn}^{0,LIQ} - H_{Sn}^{SER} = -1285.372 + 125.182498T - 28.4512\ln T$
	298.15 to 494.00	$G_{Se}^{0,HEX_A8} - H_{Se}^{SER} = -9376.371 + 174.205877T - 33.6527\ln T + 0.024243147T^2 - 15.318461 \times 10^{-6}T^3 + 102.249T^{-1}$
	494.00 to 800.00	$G_{Se}^{0,HEX_A8} - H_{Se}^{SER} = -37546.134 + 507.111538T - 81.2006585\ln T + 0.037144892T^2 - 5.611026 \times 10^{-6}T^3 + 2.614263T^{-1}$
Se LIQ.....	800.00 to 1000.00	$G_{Se}^{0,HEX_A8} - H_{Se}^{SER} = -12.193.47 + 197.770166T - 35.1456\ln T$
	298.15 to 494.00	$G_{Se}^{0,LIQ} - H_{Se}^{SER} = 50.533.347 - 1178.288242T + 194.1074389\ln T - 0.390278991T^2 + 119.219297 \times 10^{-6}T^3 - 2.224398T^{-1}$
	494.00 to 1000.00	$G_{Se}^{0,LIQ} - H_{Se}^{SER} = -5228.304 + 183.72559T - 35.1456\ln T$

Khim., 23(3), 48-51 (1968) in Russian; TR: *Moscow Univ. Chem. Bull.*, 23(3), 30-32 (1968).

70Bol: B.I. Boltaks, K.V. Perepech, P.P. Seregin, and V.T. Shipatov, "Mössbauer Study of Tin Compounds with Group VI Elements," *Izv. Akad. Nauk SSSR, Neorg. Mater.*, 6, 818-819 (1970) in Russian.

70Gla: V.M. Glazov and O.V. Situlina, "Volume Changes in the Fusion of Germanium and Tin Sulphides and Selenides," *Zh. Fiz. Khim.*, 44(8), 2018-2021 (1970) in Russian; TR: *Russ. J. Phys. Chem.*, 44(8), 1140-1143 (1970).

70Haj: S.N. Hajiev, "Advances in Experimental Thermochemistry. I. The Determination of Enthalpies of Formation of Binary Semicon-

- ducting Compounds by Direct Synthesis in a Bomb Calorimeter," *J. Chem. Thermodyn.*, 2, 765-773 (1970).
- 71Bar:** G.M. Bartenev, A.D. Tsyganov, S.A. Dembovskii, and V.I. Mikhailov, "Mössbauer-Effect Study of the Systems Sn-S and Sn-Se," *Izv. Akad. Nauk SSSR, Neorg. Mater.*, 7(8), 1442-1443 (1971) in Russian; TR: *Inorganic Mater.*, 7(8), 1280-1281 (1971).
- 71Mel:** B.T. Melekh, N.B. Stepanova, T.A. Formina, and S.A. Semenovich, "Thermodynamic Properties of Compounds in the Tin-Selenium System," *Zh. Fiz. Khim.*, 45(8), 2018-2020 (1971) in Russian; TR: *Russ. J. Phys. Chem.*, 45(8), 1144-1145 (1971).
- 74Bla1:** R. Blachnik, R. Igel, and P. Wallbrecht, "Thermodynamische Eigenschaften von Zinnchalcogeniden," *Z. Naturforsch. A*, 29, 1198-1201 (1974) in German.
- 74Bla2:** R. Blachnik and F.W. Kasper, "Tin (II) Halogenide - Tin (II) Chalcogenide Systems," *Z. Naturforsch. B*, 29, 159-162 (1974) in German.
- 76Rou:** J.-C. Rouland, B. Legendre, and C. Souleau, "The Ternary System Gold-Tin-Selenium," *Bull. Soc. Chim. Fr.*, 11-12, 1614-1624 (1976) in French.
- 77Kul:** E.A. Kulyukhina, V.P. Zlomanov, and A.V. Novoselova, "p-T Projection of the Phase Diagram of the System SnSe-Se," *Izv. Akad. Nauk SSSR, Neorg. Mater.*, 13(2), 237-240 (1977) in Russian; TR: *Inorganic Mater.*, 13(2), 200-203 (1977).
- 77Luk:** H.L. Lukas, E.T. Henig, and B. Zimmermann, "Optimization of Phase Diagrams by Least Squares Method Using Simultaneously Different Types of Data," *Calphad*, 1(3), 225-236 (1977).
- 79Wie:** H. Wiedemeier and F.J. Csillag, "The Thermal Expansion and High Temperature Transformation SnS and SnSe," *Z. Kristall.*, 149, 17-29 (1979).
- 81Bal:** L. Baldé, B. Legendre, C. Souleau, and P. Khodadad, "Heat Capacity of the Alloy $\text{Sn}_{0.5}\text{Se}_{0.5}$ in the Solid State between 375 and 1135 K," *J. Less-Common Met.*, 80, 45-50 (1981) in French.
- 81Sch:** H.G. von Schnering and H. Wiedemeier, "The High Temperature Structure of β -SnS and β -SnSe and the B16-toB33 Type λ -Transition Path," *Z. Kristall.*, 156, 143-150 (1981).
- 81Wey:** R. Wey, *Phases Transformations in Solids Minerals*, 1, Société Française de Minéralogie et de Cristallographie, Paris (1981) in French.
- 81Wie:** H. Wiedemeier, G. Pultz, U. Gaur, and B. Wunderlich, "Heat Capacity Measurements of SnSe and SnSe₂," *Thermochim. Acta*, 43, 297-303 (1981).
- 82Ale:** E.A. Aleshina, V.P. Zlomanov, and A.V. Novoselova, "Investigation of the p-T-x Diagram of the Sn-Se System," *Izv. Akad. Nauk SSSR, Neorg. Mater.*, 18(6), 913-916 (1982) in Russian; TR: *Inorganic Mater.*, 18(6), 765-767 (1982).
- 82Som1:** F. Sommer, "Association Model for the Description of the Thermodynamic Functions of Liquid Alloys. I Basic Concepts," *Z. Metallkd.*, 73, 72-76 (1982).
- 82Som2:** F. Sommer, "Association Model for the Description of the Thermodynamic Functions of Liquid Alloys. II Numerical Treatment and Results," *Z. Metallkd.*, 73, 77-86 (1982).
- 86Cha:** T. Chattopadhyay, J. Pannetier, and H.F. von Schnering, "Neutron Diffraction Study of the Structural Phase Transition in SnS and SnSe," *J. Phys. Chem. Solids*, 47(9), 879-885 (1986).
- 86Sha:** R.C. Sharma and Y.A. Chang, "The Se-Sn (Selenium-Tin) System," *Bull. Alloy Phase Diagrams*, 7(1), 68-72 (1986).
- 87Kot:** P.K. Kotchi, R. Castanet, and J.C. Mathieu, "Thermodynamic Study of the Tin-Selenium Alloys," *Z. Metallkd.*, 78(10), 714-720 (1987) in French.
- 87Ras:** S.M. Rasulov, "Temperature Dependences of the Gapwidth of $\text{Al}^{\text{IV}}\text{Se}$ and $\text{Al}^{\text{VI}}\text{Se}_3$ Semiconductors," *Izv. Akad. Nauk SSSR, Neorg. Mater.*, 23(10), 1737-1740 (1987) in Russian; TR: *Inorganic Mater.*, 23(10), 1534-1536 (1987).
- 88Kot:** P.K. Kotchi, M. Gilbert, and R. Castanet, "Thermodynamic Behaviour of the Sn-Te, Pb-Te, Sn-Se and Pb-Se Melts According to the Associated Model," *J. Less-Common Met.*, 143, L1-L6 (1988).
- 88Ras:** S.M. Rasulov, "Heat Capacity Components of Group IVA and Group VA Selenides at High Temperatures," *Teplofiz. Vys. Temp.*, 26(1), 81-86 (1988) in Russian.
- 89Cas:** R. Castanet, "Structure of Liquid Metallic Alloys From Their Thermodynamic Behaviour," *Z. Metallkd.*, 80(10), 737-744 (1989).
- 91Din:** A.T. Dinsdale, "SGTE Data for Pure Elements," *Calphad*, 15, 317-425 (1991).
- 91Ras:** S.M. Rasulov, "Vacancy Concentrations and Formation Energies for Sb_2Se_3 and SnSe," *Izv. Akad. Nauk SSSR, Neorg. Mater.*, 27(5), 1088-1090 (1991) in Russian; TR: *Inorganic Mater.*, 27(5), 914-916 (1991).
- 92Boo:** S. Boone and O.J. Kleppa, "Enthalpies of Formation for Group IV Selenides (GeSe_2 , $\text{GeSe}_2(\text{am})$, SnSe, SnSe₂, PbSe) by Direct-Combination Drop Calorimetry," *Thermochim. Acta*, 197, 109-121 (1992).
- 92Liu:** Huifang Liu and Luke L. Y. Chang, "Phase Relations in Systems of Tin Chalcogenides," *J. Alloy. Compd.*, 185, 183-190 (1992).
- 92Luk:** H.L. Lukas and S.G. Fries, "Demonstration of the Use of BINGSS With the Mg-Zn System as Example," *J. Phase Equilibria*, 13(5), 532-541 (1992).
- 94Yam:** K. Yamaguchi, K. Kameda, Y. Takeda, and K. Itagaki, "Measurements of High Temperature Heat Content of the II-VI and IV-VI (II: Zn, Cd IV: Sn, Pb VI: Se, Te) Compounds," *Mater. Trans.* 35(2), 118-124 (1994).
- 95Fra:** B. Fraisse, "Automation, Signal Treatment, X-Ray Data Recording and Thermal Analysis, Interpretation, Analysis and Data Display," Ph.D. thesis, Université des Sciences et Techniques du Languedoc, Montpellier, France (1995) in French.